Efficient Three-Axis NC Tool-Path Generation for Catmull-Clark Subdivision Surface

Jianning Zhu[1*], Xingchen Guo[1]

1 School of Mechanical Engineering, Dalian Jiaotong University, Dalian, China, 116024, China

Abstract: NC machining is one of the key technologies for application of subdivision surface in industrial fields. Excessive computer memory consumption and low efficiency of tool-path generation are two major problems, which restrict the development of high precision NC machining of subdivision surface with complex topology. To get better performance of NC machining of subdivision surface, a new method of three-axis NC tool-path generation for Catmull-Clark subdivision surface is proposed aiming at topological characteristics of Catmull-Clark subdivision surface. The basic idea of the method is to solve several problems of geometric modeling involved in NC machining of subdivision surface. First, a compact two-layer data structure is created for piecewise representation of Catmull-Clark subdivision surface. Second, a method for offset Catmull-Clark subdivision surface generation is presented based on limit mesh. Third, an efficient method for calculating intersection curve between Catmull-Clark subdivision surface and plane is presented based on divide-and-conquer strategy. Last, a method based on extracting sample vertices from limit mesh is proposed to obtain efficiently machining models of rough and semi-finish machining stages and the effect of uncut-allowance is taken into account. To validate these methods, algorithm test and machining experiments are carried out. The implementation results demonstrate that the problems of tool-path generation for subdivision surface are improved.

Keywords: Tool-Path Generation; NC machining; Subdivision Surface; Catmull-Clark Subdivision Surface/Plane Intersection; Data Structure.

1 Introduction

Subdivision surface is a new geometric modeling technology of discrete surface based on initial control mesh and certain subdivision rules. As the subdivision process proceeds, the density of vertices of control mesh becomes much higher and the subdivision surface becomes much smoother. Subdivision surface is the limit status of control mesh with a sequence of successive subdivisions in theory. Compared with NURBS (Non-Uniform Rational Basis Spline), which is wildly used in CAD/CAM area, the major advantage of subdivision surface is that it can construct smooth

* Corresponding author (47554159@qq.com)

surface of arbitrary topology easily without using the trimming and blending operations, which are computationally expensive and prone to numerical and connectivity errors. With other desirable properties such as multi-resolution, local controllability, affine invariance and global continuity etc, now subdivision surface has been widely used in many fields such as computer graphics, computer animation and geometric modeling etc. In STEP (Standard Exchange of Product data model) international standard, NURBS is the only mathematic method for geometric definition of industrial product. Trimming and blending are the two common operations used for geometric modeling of complex object based on NURBS method. However, due to some reasons numerical and connectivity errors occur in the procedure of geometric modeling, which can cause gaps especially when the model is very complex. Once such a bad CAD model is delivered to CAM system for NC machining, the quality of product will be affected directly. From the modeling point of view, subdivision surface can construct smooth model in just a single mesh patch without gaps and has better ability and higher efficiency of modeling than that of NURBS. From the manufacturing point of view, subdivision surface is more ideal for NC machining primarily because of the good performance in data conversion from CAD system to CAM system without precision-loss, while NURBS discretization is very time-consuming and will cause precision-loss. So, subdivision surface has the ability to become mainstream geometry representation method of next generation CAD/CAM system. Meanwhile, the technology of NC machining for subdivision surface is not only needed by computer film, computer animation and their surrounding industries urgently, but also offers the strong base for application of subdivision surface in other industrial fields.

In view of the situation described above, NC machining of subdivision surface is very important both in the scientific research and the market applications and has got much attention from many researchers. Kurgano et al.[1] first introduced subdivision surface to NC machining and took low-level control mesh of Catmull-Clark[2] subdivision surface as machining model. A method of tool-path generation for subdivision surface was proposed with emphasis on offset subdivision surface generation. Wu P[3] transformed Loop[4] subdivision surface to Z-map model for NC machining. In order to improve the efficiency of tool-path generation for rough machining, cover mesh was constructed as rough machining model based on low-level control mesh. In the paper[5], a method of tool-path generation for Catmull-Clark subdivision surface called S-Buffer was proposed by dividing the working area into strips and using parallel calculating environment. Lu CJ and Ting KL[6] focused on the study of machining error control in the finish machining stage. To reduce computer memory consumption, adaptive subdivision was applied to construct finish machining model. Contour-map tool-path pattern used in steep regions and iso-planar tool-path pattern used in flat regions were proposed. In the research of tool-path generation for Loop subdivision surface, Zhang ZX et al.[7] presented a machining strategy for local uncut-area based on error evaluation of machining simulation in order to improve the machining efficiency. As the key research, tool-path generation[8-11] is the foundation of many industrial applications. Commonly, the higher the precision of subdivision surface, the higher the machining

 ISSN 2572-4975 (Print), 2572-4991 (Online)

precision of product is. However, large data of high precision subdivision surface will spend a lot of computer memory consumption. Meanwhile, such huge computer memory consumption and complex topology of subdivision surface will have great effect on efficiency and quality of tool-path generation. Although some methods of NC machining for subdivision surface based on adaptive subdivision, Z-map model and S-buffer etc can reduce computer memory consumption to some extent. It is hard to improve efficiency and quality of tool-path generation further without using the unique topology structure of subdivision surface.

A complete procedure of tool-path generation for subdivision surface can be divided into several key links including subdivision surface representation, offset subdivision surface, subdivision surface intersection, tool-path planning and machining error control etc. These key links influence each other and determine together efficiency and quality of tool-path generation. Some key links which have obtained some achievements are not our focus. Compared with other discrete models, subdivision surface can be divided organically into several mesh patches with the same and regular topology structure, and such specific property is applicable to most of subdivision schemes. Aiming at the topological characteristics of subdivision surface, this paper studies tool-path generation for Catmull-Clark subdivision surface with the emphasis on subdivision surface representation, offset subdivision surface, subdivision surface intersection etc to solve the problems, which restrict the development of high precision NC machining, and achieve the goal of improving efficiency and quality of tool-path generation primarily. In section 2, Catmull-Clark subdivision surface is reviewed briefly. In section 3, a new data structure of Catmull-Clark subdivision surface is described in detail. In section 4, a method of high precision offset Catmull-Clark subdivision surface generation is presented based on limit mesh. In section 5, a method for calculating intersection curve between Catmull-Clark subdivision surface and plane is presented based on divide-and-conquer strategy. Combined with features of three-axis NC machining, in section 6, a method of three-axis tool-path generation for Catmull-Clark subdivision surface is presented. In section 7, algorithm test and machining experiments are carried out. Finally, in section 8 and section 9, discussions and conclusions are included.

2 Catmull-Clark Subdivision Surface

As an extension of the bi-cubic B-spline, Catmull-Clark subdivision surface is an approximating subdivision scheme for quadrilateral mesh, which can generates new control mesh by splitting each face into four subfaces. Let M^0 be an open or closed initial control mesh of arbitrary topology, S be Catmull-Clark subdivision operator and M^n be a control mesh after n times of subdivision. Hence, standard Catmull-Clark subdivision can be described as the linear process: $M^{n+1}=S*M^n$， n=0, 1, 2, 3…. The limit surface of Catmull-Clark subdivision scheme is C^2 continuous everywhere except at some extraordinary vertices, where it is C^1 continuous. For Catmull-Clark subdivision scheme, if the valence (number of incident edges) of an interior vertex is

four, it is a regular vertex; otherwise it is an extraordinary vertex. The new vertices of Catmull-Clark scheme can be divided into three types as below: new face-vertex (V_{f}), new edge-vertex (V_e) and new vertex-vertex (V_v). For boundary case, new boundary edge-vertex (V_{be}) and new boundary vertex-vertex (V_{bv}) also have corresponding computing methods respectively. The subdivision masks of V_{f}, V_e, V_v, V_{be} and V_{bv} for Catmull-Clark subdivision surface are shown in Figure 1(a) to (e). The new vertices are expressed by hollow dots and original vertices are expressed by solid dots.

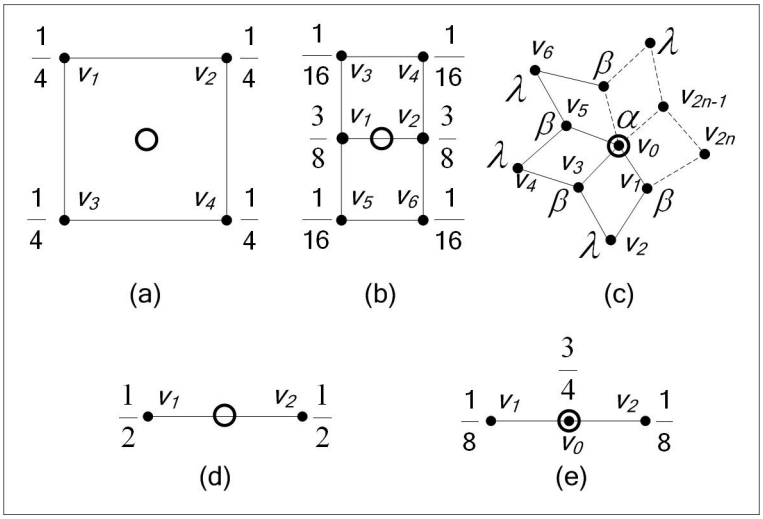

Fig. 1. Subdivision masks for Catmull-Clark subdivision surface

The computing methods of the new vertices for Catmull-Clark subdivision surface are shown as follows:

New face-vertex: V_1, V_2, V_3 and V_4 are the vertices of face as shown in Figure 1(a).

$$V_{\mathrm{f}} = \frac{V_1 + V_2 + V_3 + V_4}{4} \tag{1}$$

New edge-vertex: V_1 and V_2 are the vertices of interior edge, while V_3, V_4, V_5 and V_6 are the rest vertices of the two faces sharing the interior edge as shown in Figure 1(b).

$$V_e = \frac{3}{8}(V_1 + V_2) + \frac{1}{16}(V_3 + V_4 + V_5 + V_6) \tag{2}$$

New vertex-vertex: V_0 is the interior vertex with the valence n; V_1, V_3…, V_{2n-1} (edge points) are the rest vertices of the edges sharing V_0; V_2, V_4…, V_{2n} (face points) are the

 ISSN 2572-4975 (Print), 2572-4991 (Online)

rest vertices of the faces sharing V_0. α, β and λ are the weighting coefficients of the vertices as shown in Figure 1(c).

$$V_v = \alpha V_0 + \frac{\beta}{n}\sum_{i=1}^{n} V_{2\mathrm{i}} + \frac{\lambda}{n}\sum_{i=1}^{n} V_{2i-1} \tag{3}$$

Where $\beta = \frac{3}{2n}$, $\lambda = \frac{1}{4n}$, and $\alpha = 1 - \beta - \lambda$.

New boundary edge-vertex: V_1 and V_2 are the vertices of boundary edge as shown in Figure 1(d).

$$V_{\mathrm{be}} = \frac{V_1 + V_2}{2} \tag{4}$$

New boundary vertex-vertex: V_0 is the boundary vertex; V_1 and V_2 are the rest vertices of the two boundary edges sharing V_0 as shown in Figure 1(e).

$$V_{\mathrm{bv}} = \frac{3}{4}V_0 + \frac{1}{8}(V_1 + V_2) \tag{5}$$

As we known, subdivision surface can represent complicated object of arbitrary topology. This is mainly because the topology structure of initial control mesh is arbitrary. Although the topology structure of control mesh is globally arbitrary and irregular, under the function of certain topological rules, the topology structure of control mesh is locally simple and regular for most of subdivision schemes. For example, each quadrilateral face of initial control mesh of Catmull-Clark subdivision scheme turns into a SSP (Subdivision Surface Patch) and the topological relations between them remain unchanged after subdivision. Meanwhile, each SSP is a uniform square mesh. So, a complex subdivision surface model can be divided naturally into several simple SSPs, which can be regarded as topological characteristics of subdivision surface compared with other discrete models.

3 CELL Data Structure

As the core of subdivision surface representation, data structure is the foundation of implementation of subdivision surface as well as tool-path generation. Edge-based[12] and quad-tree[13] data structures are the most common data structures of subdivision surface. However, if the subdivision depth is too large, they will spend too much computer memory consumption and reduce efficiency of search and query because of so many pointer indirections. In the study of adaptive subdivision, V. Settgast et al.[14] constructed a data structure for representing Catmull-Clark subdivision surface based on 2D array. However due to some redundant geometrical information stored in 2D array and lack of necessary topological information, that

data structure is not beneficial to implementation of subdivision surface and tool-path generation.

In order to make up the defects, a two-layer data structure named CELL is constructed for representing Catmull-Clark subdivision surface better. The inner structure of CELL is composed by a 2D array and some 1D arrays. The 2D array named Ac, whose size is $(2N+1)^2$ at subdivision depth N, records the vertices information of SSP depicted as Ac in Figure 2. These 1D arrays, which provide the necessary information for refinement of SSP, can be classified into two types. One type named Av, whose size is 2Ne+1 at corner point's valence Ne, records the neighborhood information of corner point of SSP depicted as Av1, Av2, Av3 and Av4 in Figure 2. The other type, named Ae, whose size is 2N+1 at subdivision depth N, records the neighborhood information of boundary of SSP depicted as Ae1, Ae2, Ae3 and Ae4 in Figure 2. Half-edge data structure can be chosen as outer structure of CELL to record the topological information of initial control mesh of subdivision surface, which can demonstrate topological relations between SSPs.

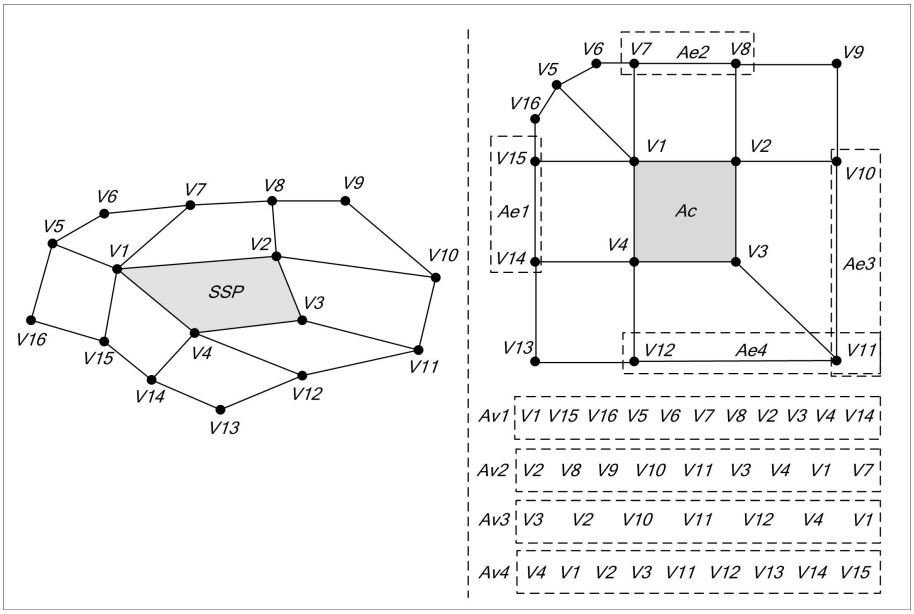

Fig. 2. Inner structure of CELL

Based on CELL, the global refinement of Catmull-Clark subdivision surface can be transformed into local refinement of SSP, which also obeys the basic subdivision rules and can be classified into three parts. The first part is the refinement of corner point of SSP, which can be generated by Av. The second part is the refinement of boundary of SSP, which can be generated by Ac and Ae. The last part is the refinement of interior of SSP, which can be generated by Ac. In order to keep refinement of SSP smoothly, the neighborhood information of SSP need to be updated. Av can be updated by itself, while Ae can be updated by Ae and Ac. In the process of refining SSP and updating

 ISSN 2572-4975 (Print), 2572-4991 (Online)

neighborhood information as shown in Figure 3, it's important to determine the type of the new vertex.

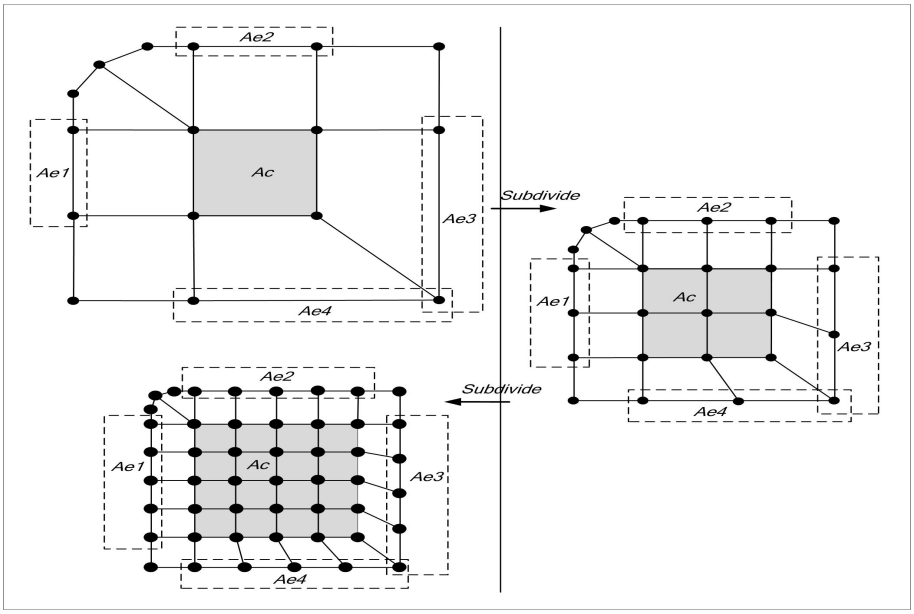

Fig.3. Refinement process with CELL

4 Offset Subdivision Surface

To compensate the radius of ball-end milling cutter, which is commonly used in three-axis NC machining, it is need to calculate offset surface in the normal direction by the radius of the ball-end milling cutter in the process of tool-path generation. The formula for calculating offset surface ($OS(u,v)$) of parametric surface ($S(u,v)$) is given:

$$OS(u,v) = S(u,v) + R * N(u,v) \tag{6}$$

Where R is the radius of ball-end milling cutter and $N(u,v)$ is the normal vector. As an important link in NC machining of subdivision surface, offset subdivision surface affects directly the precision of tool-path generation and even the quality of machining. Control mesh with a certain subdivision depth is commonly used as a substitute for limit surface in most practical applications. The methods of offset subdivision surface generation can be divided into two main categories. The first category is that, the control mesh with a certain subdivision depth is treated as general polygon, and then offset subdivision surface can be calculated based on normal vector estimation of mesh vertices. The second category is that, equation for calculating offset subdivision surface can be formed by using the relationship between control

mesh and offset control mesh. However, from the angle of calculation efficiency and precision, both of them still remain to be perfected.

The limit mesh of Catmull-Clark subdivision surface, which can be obtained by pushing the control points to their limit positions, can be used instead of control mesh for tool-path generation. The significant benefit of this approach is that high precision offset subdivision surface can be obtained efficiently based on limit position and normal vector of limit point. Furthermore, for approximating subdivision schemes such as Catmull-Clark and Loop subdivision schemes etc, the approximation precision of limit mesh is much higher than that of control mesh with the same subdivision depth. So it will reduce computer memory consumption further. Because limit mesh and control mesh have the same topology structure, limit mesh of Catmull-Clark subdivision surface also can be represented by CELL data structure. After computation of control mesh, limit mesh with the same subdivision depth can be obtained. According to Halstead M et al.[15], the formulas for calculating V^{∞} and N^{∞} of limit point are given below:

$$V^{\infty}=\frac{\mathrm{n}^2 v+4\sum_{\mathrm{i}=1}^{n} v_{2i}+\sum_{\mathrm{i}=1}^{n} v_{2i-1}}{n(n+5)} \tag{7}$$

$$\begin{cases} N^{\infty}=t_1\times t_2 \\ t_1=\sum_{i=1}^{n}(A_n C_{2i} v_{2i-1}+(C_{2i}+C_{2(i+1)})v_{2i}) \\ t_2=\sum_{i=1}^{n}(A_n C_{2(i-1)} v_{2i-1}+(C_{2(i-1)}+C_{2i})v_{2i}) \\ A_n=1+C_2+C_1\sqrt{2(9+C_2)} \\ C_i=\cos(\frac{i\pi}{n}) \end{cases} \tag{8}$$

Where v is the inner vertex of control mesh, n is the valence of v. V^{∞} and N^{∞} are the limit position and limit normal vector of v. v_1, $v_3 \ldots v_{2i-1}$ are edge points of v. v_2, $v_4 \ldots v_{2i}$ are face points of v.

5 Subdivision Surface/Plane Intersection

In three-axis NC machining, many tool-path planning methods are on the basis of calculation of intersection curve between surface and plane, especially under the condition of the plane perpendicular to the coordinate axis. The precision, efficiency and stability in calculation of intersection curve have direct effect on tool-path generation. However, many researchers treat subdivision surface as general polygon

 ISSN 2572-4975 (Print), 2572-4991 (Online)

to deal with the problems of tool-path generation using existing approaches. But these approaches are not suitable because of large data information and complex topology of subdivision model. To obtain better performance of tool-path generation, an efficient method for calculating Catmull-Clark subdivision surface/plane intersection is proposed by utilizing unique topology structure of Catmull-Clark subdivision surface. The core idea of this method is that SSP rather than subdivision surface is set as the object of intersection operation. Through calculating SSP/plane intersection and combined with divide-and-conquer strategy, subdivision surface/plane intersection can be calculated efficiently and stably. The method for calculating SSP/plane intersection mainly includes four major parts below: (1) determining whether SSP intersects plane, (2) calculating initial intersection point and determining type of intersection curve, (3) calculating following intersection points and (4) determining final intersection point.

5.1 Determining whether SSP intersects plane

If a SSP intersects a plane, it means that at least one mesh edge of the SSP intersects the plane (and vice versa). Intersection testing between mesh edge and the plane is the most basic and common approach in intersection operation. However, it is inefficient to carry out the intersection testing directly, especially when the subdivision depth is too large. In collision detection, bounding volumes are used for improving the efficiency of interference checking by using simple volume to contain more complex object. So, AABB (Axis-Aligned Bounding Box) of SSP, which can be represented by six coordinate values as below, is constructed for determining whether SSP intersects plane efficiently in our study.

$$\text{AABB } \{X_{min}, X_{max}, Y_{min}, Y_{max}, Z_{min}, Z_{max}\} \tag{9}$$

Where X_{min}, X_{max}, Y_{min}, Y_{max}, Z_{min} and Z_{max} are minimum and maximum X, Y and Z coordinate values of vertices of SSP respectively. Meanwhile, a plane perpendicular to the coordinate axis can be represented by a corresponding X, Y or Z coordinate value. So, it is easy to deduce that if the coordinate value used for representing the plane is between the corresponding minimum and maximum coordinate values used for representing the AABB, the SSP within AABB will intersect the plane. Through this approach, lots of SSPs without intersecting the plane are eliminated efficiently.

5.2 Calculating initial intersection point and determining type of intersection curve

Initial intersection point, which is expressed by a black solid dot as shown in Figure 4, is defined as the starting point of intersection curve. A searching strategy of intersection mesh edge for calculating initial intersection point based on SSP division is presented below. First, intersection testing between plane and mesh edges located in the boundary of intersection SSP are carried out. If the intersection edge, which is expressed by a yellow thicker line segment as shown in Figure 4, is found, the initial intersection point will be obtained. Otherwise, the SSP will be divided evenly into four sub-parts and then AABBs of those four sub-parts are constructed respectively.

Afterwards, at least one sub-part which intersects the plane can be determined based on corresponding coordinate values used for representing AABB and plane. Then, searching the intersection edge from boundary of that intersection sub-part is performed. Likewise, if the intersection edge is not found, the intersection sub-part will be divided evenly into four sub-parts again. And in this way, the searching scope of intersection edge will be reduced gradually until the initial intersection point is obtained.

According to topological location of the initial intersection point, the intersection curve can be divided into two types: line-type and ring-type intersection curves as shown in Figure 4. If the initial intersection point is located in the boundary of SSP, this intersection curve is line-type intersection curve; otherwise it is ring-type intersection curve.

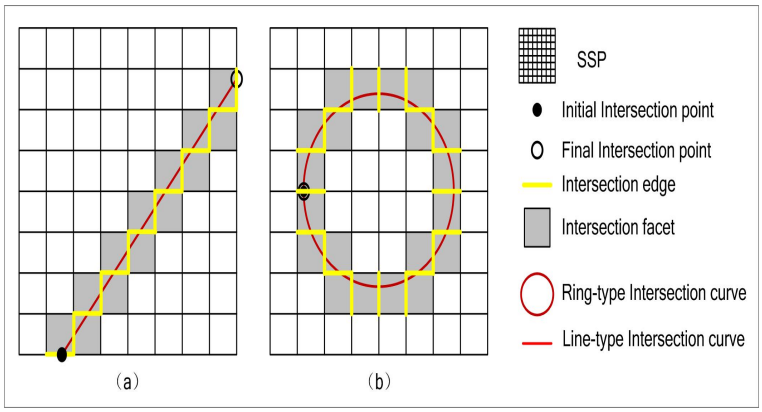

Fig.4. (a) Line-type intersection curve and (b) Ring-type intersection curve

5.3 Calculating following intersection points

All the intersection points of intersection curve except the initial intersection point can be called following intersection points. There are two basic principles for calculating the following intersection points. One is that the SSP mesh can be considered to be composed of quadrilateral faces. The other one is that if a plane intersects an edge of a quadrilateral face, it will intersect another edge of the quadrilateral face. In other words, if an intersection point between plane and quadrilateral face is known, then another intersection point, which can be defined as unknown intersection point, can be obtained. As shown in Figure 5, there are eight basic types of known intersection points between quadrilateral face and plane. Each basic type of known intersection point, which is expressed by a red solid dot as shown in Figure 5, has a corresponding set of mesh edges expressed by red thicker line segments as shown in Figure 5 for calculating the unknown intersection point. So, the unknown intersection point can be obtained as long as the known intersection point and its type are determined.

Based on above, the method for calculating following intersection points can be summarized as follows: First, the initial intersection point is set as the known

 ISSN 2572-4975 (Print), 2572-4991 (Online)

intersection point, and based on that, the intersection quadrilateral face, which is expressed by a gray face as shown in Figure 4, and the type of known intersection point are determined. Then, the intersection mesh edge can be found from the corresponding set of mesh edges, and the unknown intersection point is obtained. Last, the subsequent intersection quadrilateral face and the type of known intersection point for calculating the next following intersection point can be deduced based on the obtained intersection point. In short, all the following intersection points can be calculated recursively in the same way until the ending condition of intersection curve calculation is satisfied.

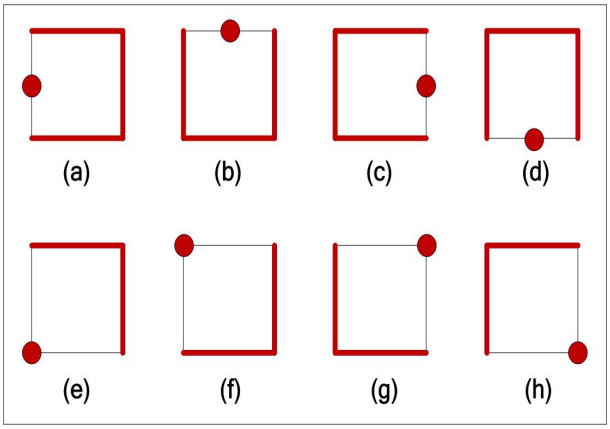

Fig.5. Eight basic types of known intersection points

5.4 Determining final intersection point

Final intersection point, which is expressed by a black hollow dot as shown in Figure 4, is defined as the ending point of the intersection curve. If a following intersection point is determined as the final intersection point, the calculation of intersection curve between SSP and plane will be stopped. A judgment will be made for determining whether the ending condition of intersection curve calculation is satisfied, whenever after calculating a following intersection point. Each type of intersection curve has its own judgment method of final intersection point. For line-type intersection curve, if the following intersection point is located in the boundary of SSP, and for ring-type intersection curve, if the following intersection point is the same as the initial intersection point, the following intersection point can be determined as the final intersection point.

After the calculation of intersection curves between all the intersection SSPs and plane are finished, all the curve segments will be merged together as a complete intersection curve based on topological relations between SSPs, which are represented by outer structure of the CELL.

6 Tool-path generation

In general, the process of NC machining of complex model can be divided into three stages: rough, semi-finish and finish machining stages, in accordance with it, each machining stage has a corresponding tool-path. Different machining stages have different emphasis on machining efficiency and machining precision, which are two main considerations of NC machining. Compared with finish machining stage, rough and semi-finish machining stages focus more on machining efficiency rather than machining precision. Aiming at this point, some approaches, most of which are based on simplified rough machining model, are presented in order to improve performance of tool-path generation. To get better performance, three approaches are presented below: 1. Combined with the idea of adaptive subdivision, all the SSPs can be subdivided independently without a unified subdivision depth. Some SSPs in the flat regions of subdivision model can ensure surface precision with a lower subdivision depth, so that the amount of data information of the machining model can be reduced. 2. In the process of subdivision depth evaluation of each SSP, not only machining error but also uncut-allowance is considered during the tool-paths generation of rough and semi-finish machining stages. Subdivision depth of some SSPs can be lower due to the impact of uncut-allowance, so that the amount of the data information of rough and semi-finish machining models can be reduced further. 3. The rough and semi-finish machining models can be obtained efficiently by a new technology named multi-resolution sampling instead of recursive calculation based on control mesh. The basic idea of multi-resolution sampling is that the data information of limit mesh with lower subdivision depth can be extracted from the limit mesh with higher subdivision depth, because original vertices of limit mesh remain unchanged as subdivision proceeds. Multi-resolution sampling interval, which is used for representing a proper interval of 2D array index between limit vertices with different subdivision depths, is the key to the implementation of the multi-resolution sampling. As shown in Figure 6, sample points expressed by red solid dots, which are extracted from limit mesh after three times of subdivision, are limit points of limit mesh after one times of subdivision, and the multi-resolution sampling interval is four.

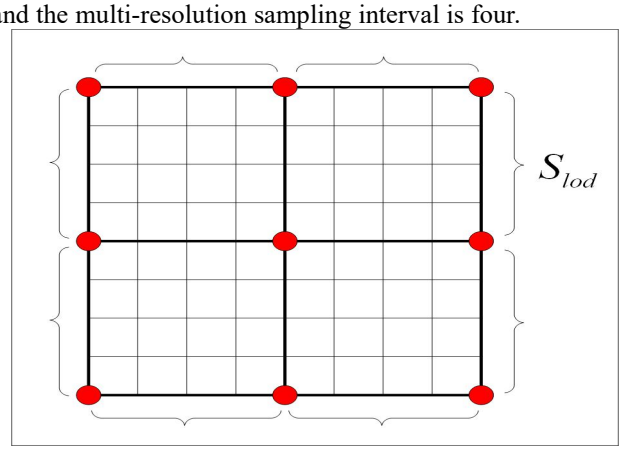

Fig. 6. Multi-resolution sampling

Multi-resolution sampling interval can be calculated as below:

 ISSN 2572-4975 (Print), 2572-4991 (Online)

$$S_{lod} = 2^{(N-M)} \tag{10}$$

Where S_{lod} is the multi-resolution sampling interval, N is the higher subdivision depth and M is the lower subdivision depth.

Based on these new methods presented in this article and some existing methods such as subdivision depth evaluation[16] and machining error control[6] etc, the process of three-axis tool-path generation for Catmull-Clark subdivision surface can described roughly as below: 1. Finish machining model is generated after subdivision depth evaluation driven by machining precision. 2. Similarly, rough and semi-finish machining models are generated by adding the uncut-allowance factor involved in subdivision depth evaluation and multi-resolution sampling. 3. Offset machining models are calculated according to geometry parameters of the selected cutter. 4. Tool-paths of each machining stage can be obtained respectively based on certain tool path pattern, machining parameters and subdivision surface/plane intersection. In the next section, an instance of three-axis tool-path generation for a subdivision surface model is shown based on methods mentioned above.

7 Algorithm test and machining experiments

We implemented our approach on Windows 7 64-bit operating system using Matlab 7.13 software and runs on an i5-3570k processor PC with 4GB RAM. A Catmull-Clark subdivision surface model (aircraft) with boundaries, whose size is 81.2mm×65.5mm×11.6mm (Length×Width×Height), is used as the test example as shown in Figure 7(b). Initial control mesh of the aircraft model with boundary edges is shown in Figure 7(a). We assumed that the finish machining precision is 0.01mm, the uncut-allowances of rough machining and semi-finish machining are 0.2mm and the size of work piece is 90mm×80mm×30mm (Length×Width×Height). Based on these, SD (Subdivision Depth) and MRSI (Multi-Resolution Sampling Interval) of each SSP can be calculated respectively. T (Time) and CMC (Computer Memory Consumption) involved in aircraft model generation and other test data including number of SSPs, maximum and minimum SD, maximum and minimum MRSI are listed in Table 1. The process of NC machining of aircraft model is divided into three stages: rough, semi-finish and finish machining stages. The cutter type, cutter size and other machining parameters including tool-path pattern, path interval and number of section planes for each machining stage are listed in Table 2. Based on these machining parameters, offset aircraft model denoted in transparent red as shown in Figure 8(b), intersection curves between section planes and aircraft model as shown in Figure 9(c), intersection curves between section planes and offset aircraft model as shown in Figure 9(d) and tool-paths of each machining stage as shown in Figure 10 can be obtained in turn. T and CMC involved in tool-paths generation of each machining stage are listed in Table 3. Machining simulations for each machining stage as shown in Figure 11 are carried out to examine the correctness of tool-paths.

Results of machining experiments for each machining stage are shown in Figure 12.

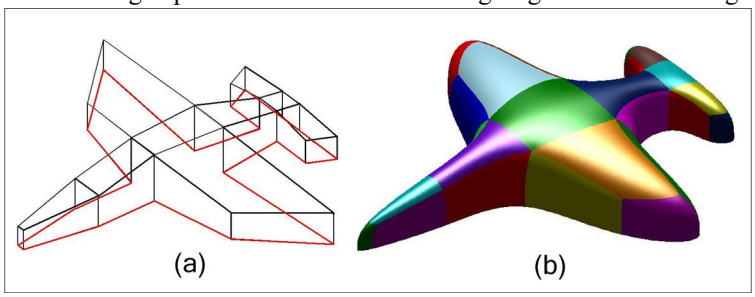

Fig. 7. (a) Initial control mesh and (b) Aircraft model

Table 1. Data of aircraft model

T (s)	CMC (MB)	Number of SSPs	Max SD	Min SD	Max MRSI	Min MRSI
71.821	276.776	29	10	7	16	4

T: time; CMC: computer memory consumption; SD: subdivision depth; MRSI: multi-resolution sampling interval

Table 2. Machining parameters for each machining stage.

Machining stage	Rough machining	Semi-finish machining	Finish machining
Cutter type	Flat-end cutter	Ball-end cutter	Ball-end cutter
Cutter size (mm)	Φ 8	R 3	R 3
Tool-path pattern	Contour-map pattern	Zig-Zag pattern	Zig-Zag pattern
Path interval (mm)	0.2	0.25	0.1
Number of section planes	90	350	872

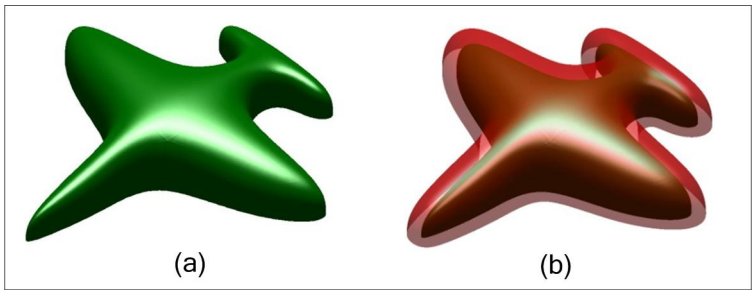

Fig.8. (a) Aircraft model (b) Offset aircraft model

 ISSN 2572-4975 (Print), 2572-4991 (Online)

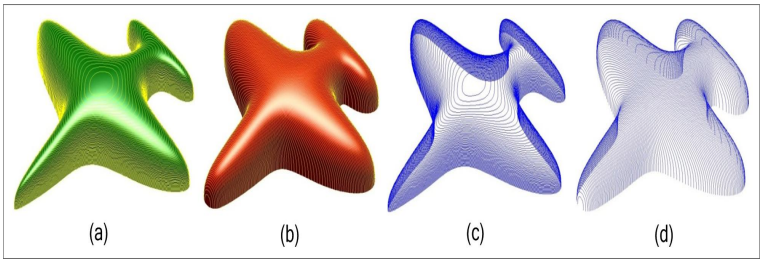

Fig. 9. (a) Aircraft model with intersection curves, (b) Offset Aircraft model with intersection curves, (c) Intersection curves, (d) Intersection curves

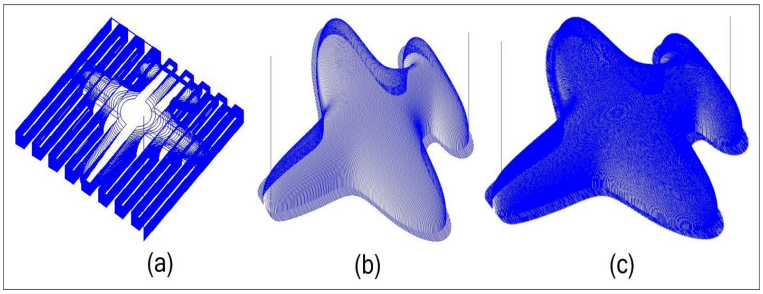

Fig. 10. Tool-paths of (a) rough machining, (b) semi-finish machining and (c) finish machining

Table 3. T and CMC of tool-path generation for each machining stage

Machining stage	T (s)	CMC (MB)
Rough machining	10.438	1.657
Semi-finish machining	17.970	8.655
Finish machining	45.954	21.818

T: time; CMC: computer memory consumption

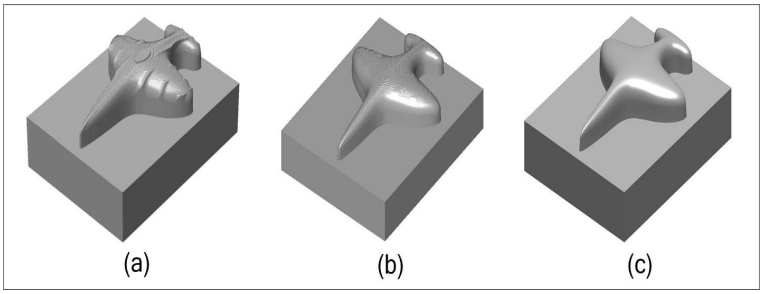

Fig.11. Simulations result of (a) rough machining, (b) semi-finish machining and (c) finish machining

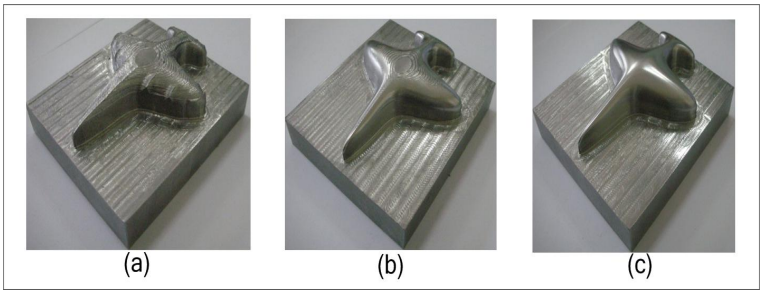

Fig. 12. Experiments result of (a) rough machining, (b) semi-finish machining and (c) finish machining

8 Discussions

8.1 Computer memory consumption

From the point of view of computer memory consumption, compared with edge-based data structures, CELL data structure can save a lot of computer memory consumption taken by topology information of subdivision surface. A quantitative analysis and comparison of computer memory consumption between CELL and half-edge data structures is carried out below. If the 64-bit version of the Windows 7 is assumed as operating system and float is used as the data type of coordinate value of vertex, the computer memory consumption taken by each pointer and vertex are 8 and 3*4 bytes respectively. Since SSP is the basic unit of subdivision surface model, Catmull-Clark SSP can be taken as the analysis object.

For CELL data structure, the computer memory consumption is taken mainly by geometric information of vertices recorded in Ac and Ae. Since the number of vertices recorded in Ac and Ae are $(2^n+1)^2$ and $4*(2^n+1)$ respectively, the computer memory consumption is $[(2^n+1)^2+4*(2^n+1)]$ *3*4 bytes for CELL data structure, n is subdivision depth. While for half-edge data structure, the computer memory consumption can be divided into two parts: one part is geometric information of vertices; another one is topology information among vertices, edges and faces. Since the number of vertices is $(2^n+1)^2$ and the number of pointers is 22 times of vertices, the total computer memory consumption is $[(2^n+1)^2*3*4+(2^n+1)^2*22*8]$ bytes for half-edge data structure, n is subdivision depth.

Then, we define $R=\frac{CMC_C}{CMC_H}$, where CMC_C and CMC_H represent the computer memory consumption taken by CELL and half-edge data structures for representing Catmull-Clark subdivision surface respectively. The value of R can be used for

 ISSN 2572-4975 (Print), 2572-4991 (Online)

performance evaluation of computer memory consumption between CELL and half-edge data structures. The smaller the value of R is, the better the performance of computer memory consumption of CELL is. As shown in Figure 13, the value of R decreases exponentially as subdivision depth increases. The value of R is less than 8% when the subdivision depth is greater than eight. In theory, the limit value of R is about 6.38% when the subdivision depth tends to infinity.

In addition, some other methods such as using limit mesh as machining model and etc are beneficial to reduce the computer memory consumption further. So, the subdivision depth of machining model and machining precision can be higher under the same hardware conditions.

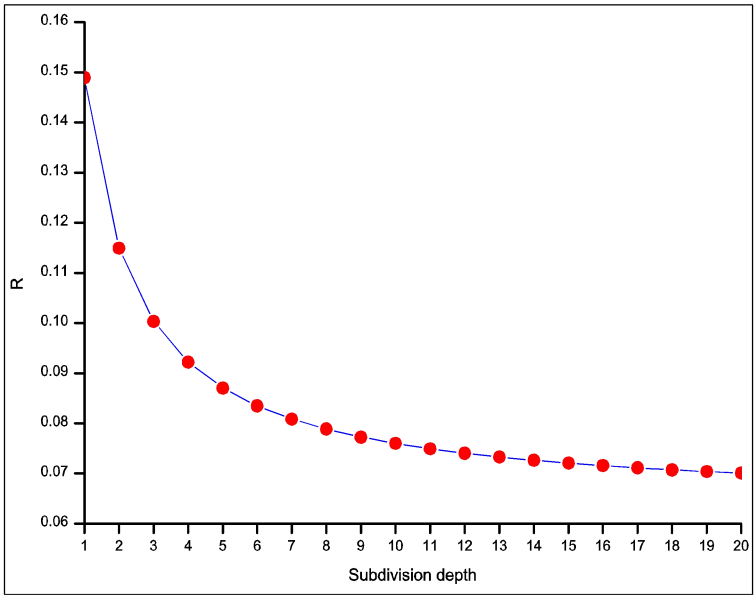

Fig.13. Comparison of computer memory consumption

8.2 Subdivision surface-based algorithm development

A proper data structure is very important for subdivision surface-based algorithm development. By combining characteristics of topology structure of Catmull-Clark subdivision surface, a two-layer data structure named CELL is proposed for piecewise Catmull-Clark subdivision surface representation. The global piecewise representation and local square topology structure are two main features of CELL data structure that are very beneficial to subdivision surface-based algorithm development.

Searching mesh vertices, edges and faces are the most basic operations for some algorithms relevant to geometric modeling and geometric properties calculation, such as surface intersection, surface trimming and distance between surfaces etc. However,

some data structures of subdivision surface, which take mesh vertex, edge or face as basic data element, are unfavorable to the efficient implementation of related algorithms under the condition of subdivision surface of complex topology and huge data information. A subdivision surface model of complex topology can be divided into several SSPs with simple and regular topology structure. And based on SSP, divide-and-conquer strategy and bounding box technique can be used to exclude irrelevant SSPs rapidly and reduce the range for searching mesh vertex, edge and face, and the efficiency and stability of related algorithms will be improved greatly.

2D array may be the best choice for Catmull-Clark SSP representation, because topological locations of mesh vertex, edge and face and topological relations between mesh vertex, edge and face can be deduced easily based on 2D array index. Due to the excellent representation ability of topological information, CELL data structure has remarkable advantages on program understanding, debugging, maintenance and testing etc. For example, in the implementation process of Catmull-Clark subdivision algorithm, the calculation of new vertices can be completed in a natural way without the neighbor searching and judgment of valence of vertex and boundary location of vertex, edge or face. Some other algorithms relevant to geometric modeling and geometric properties calculation also can be implemented efficiently by aiming at regular structure of SSP and based on the efficient search ability of CELL data structure.

9 Conclusions

By combining topological characteristics of Catmull-Clark subdivision surface and features of three-axis NC machining, an efficient method of three-axis tool-path generation for Catmull-Clark subdivision surface is presented to obtain better performance of NC machining. Computer memory consumption is reduced greatly and subdivision surface model is generated rapidly based on CELL data structure. Limit mesh, as machining model, is not only beneficial to reduce computer memory consumption further and obtain high-precision offset subdivision surface model, but also to provide the basis of multi-resolution sampling. Machining models of rough and semi-finish machining stages are obtained simply by using multi-resolution sampling technology and considering the impact of uncut-allowance. Aiming at topology structure of subdivision surface patch and combined with divide-and-conquer strategy, the method of calculating intersection curve between subdivision surface and plane is very efficient. To verify the feasibility of our method, algorithm test and machining experiments are carried out based on an airplane model. The results of algorithm test and machining experiments demonstrate that the method of tool-path generation for subdivision surface is efficient and stable. Now, the presented method is limited to three-axis NC machining, while five-axis NC machining will be the research direction in the future.

Acknowledgements

 ISSN 2572-4975 (Print), 2572-4991 (Online)

This research is supported by Guidance Planning Projects of Natural Science Foundation of Liaoning Province of China(No. 201602144), Dalian Innovation Support Program for High-level Talents(No. 2018RQ58) and Project of Research Institute of Rail Transit Equipment Technology of Colleges and Universities of Liaoning Province.

References

1. Kurgano J, Suzuki H and Kimura F, Generation of NC tool path for subdivision Surfaces, In: ***CAD/Graphics'2001,*** 2001, 676-682.
2. Catmull E and Clark J, Recursively generated B-spline surface on arbitrary topological meshes, ***Compute Aided Design***, 10 (1978) 350-355.
3. Wu P, Suzuki H and Kaze K, Three-Axis NC Cutter Path Generation for Subdivision with Z-Map, ***JSME INT J C-MECH SY,*** 48 (2005) 757-762.
4. Loop C, ***Smooth subdivision for surfaces based on triangles,*** Master's Thesis, University of Utah, USA, 1987.
5. Dai J, Wang H and Qin K, Parallel Generation of NC Tool Paths for Subdivision Surfaces, ***INT J CAD/CAM***, 4 (2004) 1-9.
6. Lu C. J. and Ting K. L., Subdivision surface-based finish machining, ***INT J PROD RES***, 44 (2006) 2445-2463.
7. Zhang Z, Maria S, Ichiro H, et al., 3-Axis NC Tool Path Generation and Machining Simulation for Subdivision Surface of Complex Models, ***INT J CAD/CAM***, 10 (2010) 1-9.
8. A Banerjee, EV Bordatchev, Effect of circular tool path on cutting force profile in micro-end-milling, ***Proc IMechE Part C: J Mech Eng Sci*****,** 226 (2012) 1589-1600.
9. N Rao, F Ismail, S Bedi, Tool path planning for five-axis machining using the principal axis method, ***INT J MACH TOOL MANU,***37(1997) 1025-1040.
10. JS Hwang, Interference-free tool-path generation in the NC machining of parametric compound surfaces, ***COMPUT AIDED DESIGN***, 24(1992) 667-676.
11. H Xiaomao, Y Chunsheng and H Yongjun, Tool path planning based on endpoint build-in optimization in rapid prototyping, ***Proc IMechE Part C: J Mech Eng Sci*** , 225 (2011) 2919-2926.
12. Kevin W, Edge-based data structures for solid modeling in curved-surface environments, ***IEEE COMPUT GRAPH***, 5(1985) 21–40.
13. Denis Z, Peter S, A unified framework for primal/dual quadrilateral subdivision schemes, ***COMPUT AIDED GEOM D***, 18(2001) 429-454.
14. Settgast V, Müller K, Fünfzig C, et al, Adaptive Tesselation of Subdivision Surfaces, ***COMPUT GRAPH*** , 28 (2004) 73-78.
15. Halstead M, Kass M, DeRose T, Efficient fair interpolation using Catmull-Clark surfaces, In: ***SIGGRAPH '93 Proceedings of the 20th annual conference on Computer graphics and interactive techniques*****,** 35-44.
16. Huang Z, Deng J, Wang G, A bound on the approximation of a Catmull–Clark subdivision surface by its limit mesh, ***COMPUT AIDED GEOM D***, 25 (2008) 457-469.